Design and Implementation of a Water Tank Control System Employing a MIMO PID Controller

Arturo Rojas–Moreno and Arturo Parra–Quispe
Faculty of Electrical and Electronic Engineering, National University of Engineering
Lima, Lima 25, Peru

ABSTRACT

This paper develops a design procedure of a MIMO PID (Multi-Input-Multi-Output Proportional–Integral–Derivative) control system for controlling level and temperature in a water tank plant. Such a plant can be described by interconnected nonlinear differential equations, which could complicate the analytical aspects of modeling and controller design. However, a linearized technic was applied to obtain a MIMO linear description, which permit to configure a control system by combining a linear MIMO PID controller acting on the water tank plant. Experimental results demonstrate that the designed controller is able to stabilize tank level and temperature simultaneously. The control software was written in LabVIEW code.

Keywords: Water tank plant, nonlinear modeling, MIMO PID controller, control software, LabVIEW code.

1 INTRODUCTION

Water tank system are being used to illustrate both traditional and advanced multivariable control strategies. Quantitative Feedback Theory is employed in [1] to design a robust controller to regulate the liquid level in two coupled glass tanks. A multivariable laboratory process of four interconnected water tanks is considered in [2] for modeling and robust control of the tank level. In [2], flow and temperature of a water tank system are controlled employing a backstepping method, whereas a four tank system laboratory experiment is designed in [4] to illustrate the effects that time-varying dynamics can have on controllability. Also, predictive fuzzy modeling technique is employed in [5] for analysis of a closed water tank, and an Internal Mode Contro–based robust tunable controller design technique is applied to a water tank control system in [6].

Regulation of the level of liquid in a tank is a common industrial process control problem. The modeling of the dynamics of the liquid level and flow rate relies on the approximate linearity at the equilibrium point. A linear fractional transformation framework is set up for robust control design, in which the nonlinearity is considered as model uncertainty. An IMC–based robust tunable controller design technique is applied to a water tank control system. As the design provides an on-line tuning method, the controller can be adjusted when the operating point changes. Experimental results show the advantages of this design.

The study developed in this paper considers a water tank system described by interconnected nonlinear differential equations. The objective control consist in stabilize level and temperature of the water tank simultaneously employing a MIMO PID controller.

2 MODELING THE PLANT

Fig. 1 depicts the water tank plant studied here. In such a plant, cold water is sent to the tank, heated electrically, and sent out. The plant is a MIMO type because possesses two control inputs: the inflow rate and the heater supply, and two controlled outputs: water level and the temperature in the tank. Table 2 describes all variables and valued parameters of the plant into consideration.

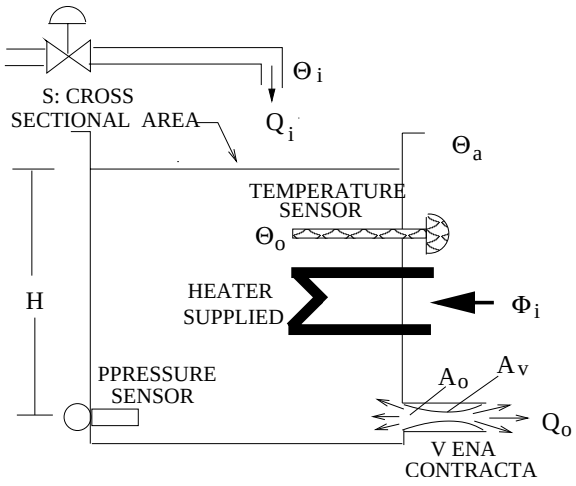

Fig. 1: Water tank plant.

Table 1: Variables and valued parameters of the water tank plant.

Symbol	Description and value
d_S	tank diameter = 0.25 m
S	tank cross sectional area = 0.041 m^2
$\overline{H}$	water level in steady state = 0.19 m
H	water level
h	residual $h = H - \overline{H}$
Q_i	tank inflow rate
$\overline{Q}_i$	inflow rate in steady state = 0.16 m^3/h
q_i	residual $q_i = Q_i - \overline{Q}_i$
Q_o	tank outflow rate
q_o	residual $q_o = Q_o - \overline{Q}_o$
R_h	hydraulic resistance $R_h = \frac{\overline{H}}{\overline{Q}} = 2700\ \frac{s}{m^2}$
g	gravitational constant = 9.81 m/s^2
ρ	water density =1000 kg/m^3
d_o	output orifice diameter = 0.0127 m
A_o	orifice cross sectional area = 0.000126 m^2
A_v	vena cross sectional area = m^2
C_c	area correction between A_o and A_v
C_v	frictional losses correction = 0.8 to 0.99
C_d	discharge coefficient $C_d = C_v C_c = 0.5$
a	discharge factor $a = 0.00028\ \frac{m^{2.5}}{s}$
C_p	water specific heat = 4186.8 $\frac{J}{kg\,K}$
R_t	termal resistance $R_t = \frac{1}{C_p \rho \overline{Q}} = 0.0054\ \frac{K}{W}$
Θ_a	atmosphere temperature = 27.0 ^{o}C
$\overline{\Theta}_o$	steady state tank temperature = 31 ^{o}C
Θ_o	outflow rate temperature
θ_o	residual $\theta_o = \Theta_o - \overline{\Theta}_o$
Φ_i	heater supplied
$\overline{\Phi}_i$	steady state heater supplied = 1540 W
Φ_T	water heat in the tank
Φ_o	outflow rate heat
Φ_s	released heat $\Phi_s = \frac{\Theta_o - \Theta_a}{R_t}$
Φ_c	inflow rate heat

The rate of water outflow is expressed by

$$S\frac{dH}{dt} = S\dot{H} = Q_i - Q_o \tag{1}$$

where the flow rate through the orifice is [7]

$$Q_o = C_v C_c A_o \sqrt{2gh} = C_d A_o \sqrt{h} = a\sqrt{h} \tag{2}$$

where $a = C_d A_o \sqrt{2g}$ is the discharge factor, C_c is the area correction between A_o and A_v (see figure 1)

$$A_v = C_c A_o$$

and C_v is a coefficient that considers frictional losses through the orifice. The product $C_d = C_v C_c$, the discharge coefficient, can be determined experimentally for a given orifice. Values of C_c vary between 0.6 and 1.0, while C_v can take values between 0.8 and 0.99. Therefore

$$0.48 \leq C_d \leq 0.99 \tag{3}$$

We assume a value C_d =0.5. From (1), we obtain the first state equation

$$\dot{H} = -\frac{a}{S}\sqrt{H} + \frac{1}{S}Q_i \tag{4}$$

On the other hand, assuming that the water temperature in the tank is uniform, the heat balance is formulated as [3]

$$\Phi_T = -\Phi_o - \Phi_s + \Phi_c + \Phi_i \tag{5}$$

where Φ_T is the water heat in the tank, Φ_o is the outflow heat, Φ_s is the heat released to the air, Φ_c is the inflow heat, and Φ_i is the heater supplied. Also

$$\Phi_T = S\rho C_p \frac{Q_o^2}{a^2}\frac{d\Theta_o}{dt} = S\rho C_p H \frac{d\Theta_o}{dt} \tag{6}$$

$$\Phi_o = C_p \rho \Theta_o Q_o = C_p \rho a \Theta_o \sqrt{H} \tag{7}$$

$$\Phi_s = \frac{\Theta_o - \Theta_a}{R_t} \tag{8}$$

$$\Phi_c = C_p \rho \Theta_i Q_i \tag{9}$$

The second state equation is obtained by solving for $\frac{d\Theta_o}{dt} = \dot{\Theta}_o$ the equation (5)

$$\dot{\Theta}_o = -\frac{a}{S}\frac{\Theta_o}{\sqrt{H}} - \frac{\Theta_o - \Theta_a}{S\rho C_p R_t H} + \frac{\Theta_i}{A}\frac{Q_i}{H} + \frac{1}{S\rho C_p}\frac{\Phi_i}{H} \tag{10}$$

Linearizing equations (4) and (4) for the operation point $(\overline{H}, \overline{\Theta}_o)$ using Jacobian matrices leads to

$$\begin{aligned} \dot{\mathbf{x}} &= \mathbf{A}\mathbf{x} + \mathbf{B}\mathbf{u} \\ \mathbf{y} &= \mathbf{C}\mathbf{x} = \begin{bmatrix} 1 & 0 \\ 0 & 1 \end{bmatrix}\mathbf{x} \end{aligned} \tag{11}$$

$$\mathbf{A} = \begin{bmatrix} \frac{\partial f_1}{\partial H} & \frac{\partial f_1}{\partial \Theta_0} \\ \frac{\partial f_2}{\partial H} & \frac{\partial f_2}{\partial \Theta_0} \end{bmatrix} \qquad \mathbf{B} = \begin{bmatrix} \frac{\partial f_1}{\partial Q_i} & \frac{\partial f_1}{\partial \Phi_i} \\ \frac{\partial f_2}{\partial Q_i} & \frac{\partial f_2}{\partial \Phi_i} \end{bmatrix}$$

where $f_1 = \dot{H}$ and $f_2 = \dot{\Phi}_o$ are equations (4) and (10) respectively, and the residual state and control vectors $\mathbf{x} = [h \quad \theta_o]^T$ and $\mathbf{u} = [q_i \quad \Phi_o]^T$ are defined by

$$\begin{bmatrix} h \\ \theta_o \end{bmatrix} = \begin{bmatrix} H - \overline{H} \\ \Theta_0 - \overline{\Theta}_0 \end{bmatrix} \qquad \begin{bmatrix} q_i \\ \Phi_o \end{bmatrix} = \begin{bmatrix} Q_i - \overline{Q}_i \\ \Phi_0 - \overline{\Phi}_0 \end{bmatrix} \tag{12}$$

Performing partial derivatives on (11) produces

$$\begin{aligned} \frac{\partial f_1}{\partial H} &= -\frac{a}{2S\sqrt{\overline{H}}} & \frac{\partial f_1}{\partial \Theta_o} &= 0 \\ \frac{\partial f_2}{\partial H} &= \frac{a}{2S}\frac{\overline{\Theta}_o}{\sqrt{\overline{H}^3}} + \frac{\overline{\Theta}_o - \theta_a}{S\rho C_p R_t \overline{H}^2} - \frac{\theta_i \overline{Q}_i}{S\overline{H}^2} - \frac{\overline{\Phi}_i}{S\rho C_p \overline{H}^2} & & \\ \frac{\partial f_2}{\partial \Theta_o} &= -\frac{a}{S\sqrt{\overline{H}}} - \frac{1}{S\rho C_p R_t \overline{H}} & & \\ \frac{\partial f_1}{\partial Q_i} &= \frac{1}{S} & \frac{\partial f_1}{\partial \Phi_i} &= 0 \\ \frac{\partial f_2}{\partial Q_i} &= \frac{\theta_i}{S\overline{H}} & \frac{\partial f_2}{\partial \Phi_i} &= \frac{1}{S\rho C_p \overline{H}} \end{aligned} \tag{13}$$

3 MIMO PID CONTROLLER DESIGN

Figure 2 shows the block diagram of a MIMO PID control system where $\mathbf{G}_s(s)$ is the MIMO PID controller, $\mathbf{R}$ is the vector of desired outputs, $\mathbf{Y} = \mathbf{G}_p(s)\mathbf{U}$ (s is the Laplace variable), and $\mathbf{U} = \mathbf{G}_s(s)[\mathbf{R} - \mathbf{Y}]$. Therefore

$$\begin{aligned} \mathbf{G_c}(s) &= (\mathbf{I} + \mathbf{G}_p(s)\mathbf{G}_s(s))^{-1}\mathbf{G}_p(s)\mathbf{G}_s(s) \\ &= \begin{bmatrix} G_{c11}(s) & G_{c12}(s) \\ G_{c21}(s) & G_{c22}(s) \end{bmatrix} \end{aligned} \quad (14)$$

$$\begin{aligned} \mathbf{G_s}(s) &= \mathbf{G}_p(s)^{-1}\mathbf{G}_c(s)(\mathbf{I} - \mathbf{G}_c(s))^{-1} \\ &= \begin{bmatrix} G_{s11}(s) & G_{s12}(s) \\ G_{s21}(s) & G_{s22}(s) \end{bmatrix} \end{aligned} \quad (15)$$

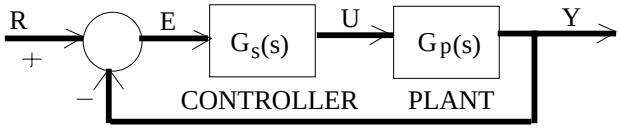

Fig. 2: Block diagram of a MIMO PID control system.

The MIMO PID control system studied here must satisfy the following performance specifications [8]

1) No interaction between reference inputs $\mathbf{R}$ (the desired outputs) and outputs $\mathbf{Y}$.
2) Static accuracy.
3) Stability
3) Insensitivity to disturbances

No Interaction
To obtain complete decoupling between vectors $\mathbf{R}$ and $\mathbf{Y}$, matrix $\mathbf{G}_c$ (equation (14)) must be diagonal, which means transfer functions $G_{c12}(s)$ and $G_{c21}(s)$ are null. A necessary and sufficient condition for noninteraction is that the open–loop transfer matrix $\mathbf{G}(s) = \mathbf{G}_p(s)\mathbf{G}_s(s)$ also be diagonal. This fact is easy to prove. Using (14)

$$\mathbf{G}(s) = \mathbf{G}_c(s)[\mathbf{I} - \mathbf{G}_c(s)]^{-1}$$

Since $\mathbf{G}_c(s)$ is diagonal, then matrix $[\mathbf{I} - \mathbf{G}_c(s)]$ and its inverse are also diagonal

$$[\mathbf{I} - \mathbf{G}_c(s)]^{-1} = \begin{bmatrix} \frac{1}{1-G_{c11}(s)} & 0 \\ 0 & \frac{1}{1-G_{c22}(s)} \end{bmatrix} \quad (16)$$

Therefore

$$\mathbf{G}(s) = \begin{bmatrix} \frac{G_{c11}(s)}{1-G_{c11}(s)} & 0 \\ 0 & \frac{G_{c22}(s)}{1-G_{c22}(s)} \end{bmatrix} \quad (17)$$

Static Accuracy
To achieve static accuracy, the vector error

$$\mathbf{E} = \mathbf{R} - \mathbf{Y} = [\mathbf{I} - \mathbf{G}_c(s)]\mathbf{R}$$

for constant step–type $\mathbf{R}$ should approach to zero

$$\lim_{t\to\infty} \mathbf{E} = \mathbf{0}$$

Applying the final–value theorem, a necessary condition for zero static accuracy is

$$\lim_{s\to 0} \mathbf{G}_c(s) = \mathbf{I} \quad (18)$$

On using condition (18) into (14) produces

$$\lim_{s\to 0}[\mathbf{I} + \mathbf{G}(s)] = \lim_{s\to 0} \mathbf{G}(s) \quad (19)$$

which implies that $[\mathbf{I} + \mathbf{G}(0)] = \mathbf{G}(0)$, meaning that each diagonal element of $\mathbf{G}$ should approach to ∞ for $s = 0$. Therefore, each diagonal element of $\mathbf{G}$ must contain at least one integrator.

Stability
To preserve stability of the designed control system, all eigenvalues of its characteristic equation $det[\mathbf{I}+\mathbf{G}(s)] = 0$ must be located on the left side of the s plane [8]. Since

$$\mathbf{I} + \mathbf{G}(s) = \begin{bmatrix} 1 + G_{11}(s) & 0 \\ 0 & 1 + G_{22}(s) \end{bmatrix} \quad (20)$$

then

$$det[\mathbf{I} + \mathbf{G}(s)] = (1 + G_{11}(s))(1 + G_{22}(s)) = 0$$

implying that $(1 + G_{11}(s) = 0)$ and $(1 + G_{22}(s)) = 0$.

Insensitivity to disturbances
By setting $\mathbf{R} = \mathbf{0}$ and introducing a vector disturbance $\mathbf{Z}$ in figure 2, this turns into the block diagram showed in figure (3) which can be used to compute the effect of disturbances in output vector $\mathbf{Y}$ as follows

$$\mathbf{Y} = (\mathbf{I} + \mathbf{G}_p\mathbf{G}_s)^{-1}\mathbf{G}_p\mathbf{Z} = (\mathbf{I} + \mathbf{G}(s))^{-1}\mathbf{G}_p\mathbf{Z} \quad (21)$$

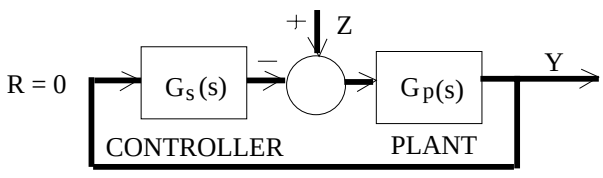

Fig. 3: Block diagram for computing the effect of the disturbances.

4 MIMO CONTROLLER CALCULATION

The transfer matrix $\mathbf{G_p}(s)$ of the linear plant model given by (11) can be calculated from

$$\mathbf{G_p}(s) = \mathbf{C}(s\mathbf{I} - \mathbf{A})^{-1}\mathbf{B} \tag{22}$$

$$\mathbf{G_p}(s) = \begin{bmatrix} \frac{K_{p11}}{T_{p11}s+1} & 0 \\ \frac{Ps+Q}{(T_{p11}s+1)(T_{p22}s+1)} & \frac{K_{p22}}{T_{p22}s+1} \end{bmatrix}$$

where s is the Laplace variable, $\mathbf{I}$ is the identity matrix, and K_{p11}, K_{p22}, P and Q are constants.

To determine the control matrix $\mathbf{G}_s(s)$ given by (15), it is required to specify the diagonal form of the closed–loop transfer matrix $\mathbf{G}_c(s)$. We may attempt the following choice

$$\mathbf{G_c}(s) = \begin{bmatrix} \frac{1}{T_{niv}s+1} & 0 \\ 0 & \frac{1}{T_{temp}s+1} \end{bmatrix} \tag{23}$$

due to the following reasons

1) $\mathbf{G_c}(s)$ is diagonal, satisfying the non interaction requirement.
2) $\mathbf{G_c}(0) = \mathbf{I}$, fulfilling the static accuracy requirement stipulated in (18).
3) Knowing that $\mathbf{Y} = \mathbf{G}_c\mathbf{R}$, then the two channels of the system have the form

   $$Y_1 = \frac{1}{T_{niv}s+1}R_1 \qquad Y_2 = \frac{1}{T_{temp}s+1}R_2$$

   As $\mathbf{R}$ is assuming to be a step–type vector, the level channel $Y1$ and the temperature channel Y_2 will reach exponentially to their correspondence references R_1 and R_2. Observe that T_{niv} and T_{temp} are the time constants of the channels.
4) Using (17), $\mathbf{G}(s) = \mathbf{G}_p(s)\mathbf{G}_s(s)$ is found to be

   $$\mathbf{G}(s) = \begin{bmatrix} \frac{T_{niv}}{s} & 0 \\ 0 & \frac{T_{temp}}{s} \end{bmatrix} \tag{24}$$

   By application of the final value theorem in (21), assuming that $\mathbf{Z}$ is a step–type disturbance, it is easy to demonstrate that

   $$\lim_{s\to 0}\{[\mathbf{I} + \mathbf{G}(s)]^{-1}\mathbf{G}_p\mathbf{Z}\} = \mathbf{0}$$

   This result satisfies the requirement of insensitivity to disturbances.

The control matrix $\mathbf{G_s}(s)$ is obtained using (15):

$$\mathbf{G_s}(s) = \begin{bmatrix} G_{s11}(s) & 0 \\ G_{s21}(s) & G_{s22}(s) \end{bmatrix} \tag{25}$$

$$= \begin{bmatrix} -K_{s11}\left(1 + \frac{1}{T_{I11}\,s}\right) & 0 \\ -K_{s21}\left(1 + \frac{1}{T_{I211}\,s}\right) & -K_{s22}\left(1 + \frac{1}{T_{I221}\,s}\right) \end{bmatrix}$$

Observe that $\mathbf{G_s}(s)$ possess three PI controllers, one of them negative. Figura 4 the block diagram of the MIMO PID control system for controlling the water tank plant.

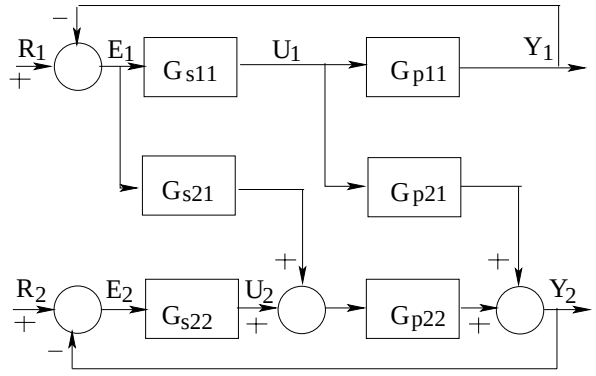

Fig. 4: Block diagram of the MIMO PID control system.

5 HARDWARE AND SOFTWARE

Hardware

Fig.5 depicts the hardware configuration of the water tank control system, which includes level measurement using a Valcom pressure sensor (range: [0, 1.25] m) and a Safir type P transmitter with digital indicator set to [0, 10] V, temperature measurement using a Pt 100 RTD sensor (range: [0 ^{o}C/4 mA, 100 ^{o}C/20 mA]) and a Safir type T transmitter with digital indicator which converts [4, 20] mA to [0, 10] V, a Sauter AVM104S valve with electric drive (range: [0, 10 V]) to regulate the inflow rate of water, a SPC1-35 power controller with input set to [1, 5] V connected to an electric resistance for water heating, a NI PCI 6229 data acquisition card allocated in a Pentium PC, and the water tank plant.

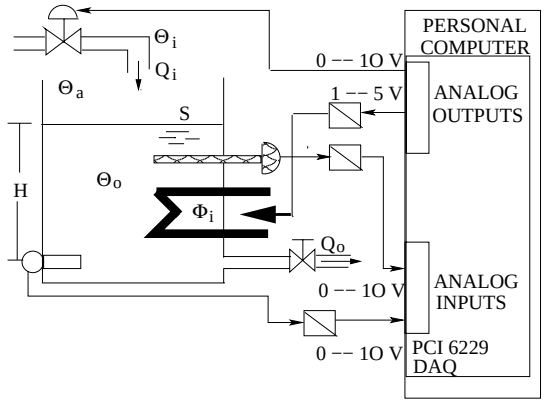

Fig. 5: Hardware configuration of the water tank control system.

Control Software

The MIMO PID control algorithm was written in LabVIEW code (V 8.5) and executed in the CPU of the PC. Such an algorithm process level and temperature signals and generate two control signals, one for the valve and another for the power controller. Actually, the MIMO PID controller given by (25) requires three PI control algorithms. The basic form of a PID control algorithm is

$$\begin{aligned} u(t) &= K_p e(t) + \frac{K_p}{T_i}\int_0^t e(t)d\tau + K_p T_d \frac{de(t)}{dt} \\ &= P(t) + I(t) + D(t) \\ e(t) &= r(t) - y(t) \end{aligned} \tag{26}$$

where $u(t)$, $y(t)$, $e(t)$, and $r(t)$ are the control, output, error and set–point signals, respectively. Also, K_p, T_i, and T_d represent the proporcional gain, the integral time, and the derivative time, respectively. That basic PID algorithm has been modified as to improve its performance.

To prevent drastic changes in the derivative term $D(t)$ due to abrupt changes in $r(t)$, let us the derivative action operate only on $y(t)$ and not on $r(t)$, that is

$$D(t) = -K_p T_d \frac{dy(t)}{dt}$$

It is advisable to filter the pure derivative term $\frac{dy(t)}{dt}$ employing a first order filter to limit the high frequency measurement noise amplification in $y(t)$, that is

$$D(s) = -\frac{K_p T_d\, s}{1 + T_f\, s} y(s) \qquad T_f = \frac{T_d}{N} \tag{27}$$

where T_f is a time constant and N is the bound of the derivative gain (a value between 3 and 10).

The control software is written in the discrete–time domain. So we need a discrete form of the modified PID controller. Being $k = \frac{t}{T}$ the discrete time, where T is the sampling time, $P(t)$ takes the form

$$P(k) = K_P\, e(k)$$

We can employ trapezoidal approximation for the integral term $I(t)$

$$I(k) = \frac{K_p}{T_i}\sum_{i=1}^{k} T\frac{[e(i) + e(i-1)]}{2} =$$

$$\frac{K_p}{T_i}\sum_{i=1}^{k-1} T\frac{[e(i) + e(i-1)]}{2} + \frac{K_p}{T_i} T\frac{[e(k) + e(k-1)]}{2}$$

For the discrete time $(k-1)$ holds

$$I(k-1) = \frac{K_p}{T_i}\sum_{i=1}^{k-1} T\frac{[e(i) + e(i-1)]}{2}$$

Subtracting $I(k-1)$ from $I(k)$ we obtain the recursive form of $I(k)$

$$I(k) = I(k-1) + \frac{K_p\, T}{2T_i}[e(k) + e(k-1)] \tag{28}$$

The derivative term given by (27) can be rewritten as

$$D(t) + T_f\, \dot{D}(t) = -K_p T_d\, \dot{y}(t)$$

Performing backward approximation of the derivative terms

$$\dot{D}(t) \simeq \frac{D(k) - D(k-1)}{T} \qquad \dot{y}(t)\frac{y(k) - y(k-1)}{T}$$

leads to

$$D(k) = \frac{T_d}{NT + T_d}\left\{D(k-1) - K_p N[y(k) - y(k-1)]\right\} \tag{29}$$

The designed control signal $u(k)$ is limited to be between u_{min} and and u_{max} before entering to the actuator: the PWM amplifier. It may happen that $u(k)$ reaches such limits. When this happens the feedback loop is broken and the system runs as an open loop because the actuator will remain at its limit independently of the process output $y(k)$. Meanwhile, the $I(k)$ term of the controller may become very large or, in other words, it "winds up" because the error will be continuously integrated. To avoid this integral windup phenomena, it is recommended to turn off the integral action as soon as the actuator saturates. One way to turn off the integral term is to use a dead zone

$$v(k) = P(k) + D(k) + I(k)$$

$$u(k) = \begin{cases} P(k) + \frac{K_P}{T_i} + D(k), & v(k) \le u_{min} \\ v(k), & u_{min} \le v(k) \le u_{max} \\ P(t) + \frac{K_P}{T_i} + D(k), & v(k) \ge u_{max} \end{cases}$$

On the other hand, when the controller conmutes from manual to automatic operation, the control signal $u(t)$ may change ("bump") from a value to another independent of the value of the error signal $e(t)$. To obtain bumpless operation of the controller, the control algorithm must be also executed in manual operation. Fig. 6 pictures a portion of the control software written in LabVIEW code [9], [10].

6 EXPERIMENTAL RESULTS

Figure 7 depicts the controlled level and its corresponding control action (the inflow rate), while figure 8 shows the controlled temperature and its corresponding control action (the heat supplied). Constants and time constants of the MIMO controller (see relation (25) were set to $K_{s11} = 4$, $K_{s21} = 4$, $K_{s22} = 6$, $T_{i11} = 100$, $T_{i21} = 100$ and $T_{i22} = 100$. Reference points level and

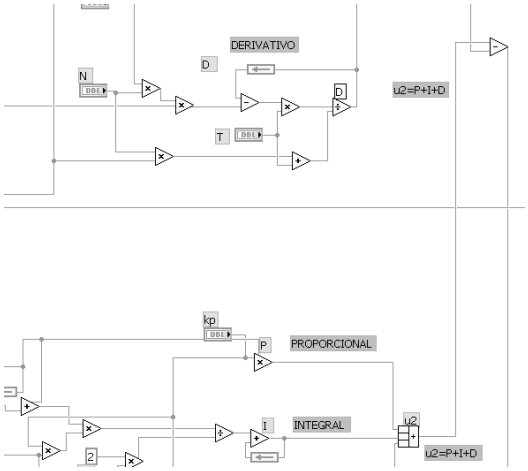

Fig. 6: Portion of the control software.

temperature were set to 19 cm and 31^{o}C, respectively. The sampling period used to execute the algorithm was 1 s. We observe that the designed MIMO control algorithm is able to stabilize the controlled outputs with sufficient speed.

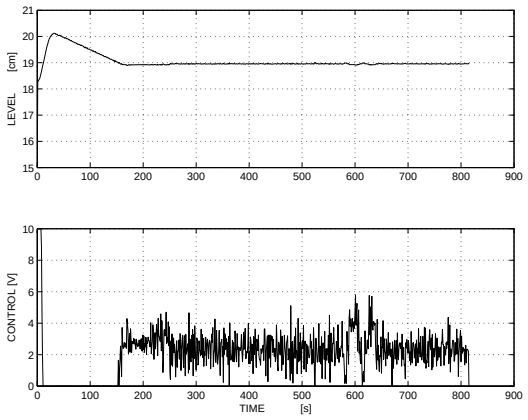

Fig. 7: Controlled tank level and its corresponding control force.

7 CONCLUSIONS

In light of the experimental result, we may assure that it is possible to find an interconnected MIMO linear dynamic model of the water tank plant capable of capturing significant features of the actual MIMO interconnected nonlinear plant. Such a model permit to design and implement a MIMO PID linear controller, capable of stabilizing the outputs of the plant (level and temperature) in real–time operation.

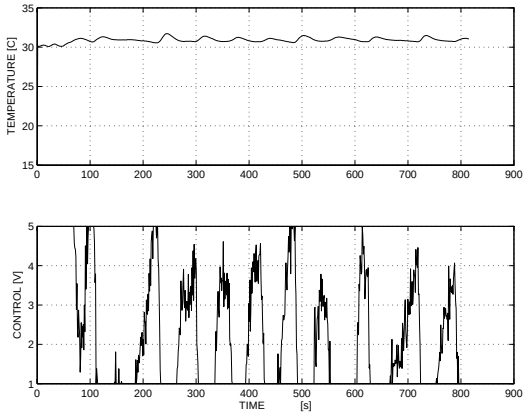

Fig. 8: Controlled tank temperature and its corresponding control force.

8 REFERENCES

[1] Pratibha Shingare, and M. A. Joshi, "Modeling and Robust Control of Level in Hybrid Tanks", **Proceedings of the World Academy of Science, Engineering and Technology**, Vol 20, April 2007.

[2] Rajanikanth Vadigepalli, Edward P. Gatzke and Francis J. Doyle III, "Robust Control of a Multivariable Experimental Four-Tank System", **Industrial and Engineering Chemistry Research**, 2001; 40 (8).

[3] Jin-Hua She, Hiroshi Odajima, Hiroshi Hashimoto and Minoru Higashiguchi, "Flow and temperature control of a tank system by backstepping method, **The Fourth International Conference on Motion and Vibration Control**, ETH Zurich, Switzerland, August 25-28, 1998, pp 449-454.

[4] Effendi Rusli, Siong Ang, and Richard D. Braatz, "A Quadruple Tank Process Control Experiment", **Journal of Chemical Engineering Education**, Vol 38, Number 3, 2004.

[5] Raimundas Liutkeviius and Saulius Dainys, " Hybrid Fuzzy Model of a Nonlinear Plant", **Information Technology and Control**, Vol.34, No.1, 2005.

[6] Y. Duan, B. Boulet, and H. Michalska, "Application of IMC-based Robust Tunable Controller Design to Water Tank Level Regulation", **Proceeding (550) Modelling, Identification, and Control**, Insbruck, Austria, Feb. 2007.

[7] W. F. Hughes and J. A. Brighton, **Theory and Problems of Fluid Dynamics**, Shaum's outline series, McGraw-Hill, 2nd edition, Inc., 1991.

[8] Olle I Elgerd, **Control Systems Theory**, McGraw-Hill Kogakusha. LTD., Tokyo at. al., 1967.

[9] **LabVIEW Fundamentals**, National Instruments, August 2007, 324029C–01.

[10] **Getting Started with LabVIEW**, National Instruments, August 2007, 323427D–01.